DSA Preparation of Pt NPs @MIL-53(Fe) and Its Catalytic Behaviors

Li, Yafeng*[+]; Ni, Siyu; Wang, Zhen; Lu, Jinjjing
School of Chemical Engineering, Changchun University of Technology, 130012, Changchun, P. R. CHINA

Zhang, Limei
Computer Science and Engineering College, Changchun University of Technology, 130012, Changchun, P. R. CHINA

ABSTRACT: *In this work, the effects of preparation methods such as CE oven, microwave irradiation and ultrasound on the morphology, particle size and crystallinity of MIL-53(Fe) are firstly investigated. Furthermore, the methods are utilized to prepare Pt NPs@MIL-53(Fe). As a result, well-defined Pt NPs@MIL-53(Fe) prepared by microwave irradiation exhibits uniformed morphology, high crystallinity, and high-disperse Pt NPs, which has been confirmed by FT-IR, TG, N_2 adsorption at 77K, TEM and PXRD. Pt NPs@MIL-53(Fe) composite can selectively catalyze the thiophene hydrogenation over nitrobenzene and benzothiophene hydrogenation. The result shows that the sulfur amount can rapidly be reduced to less than 10 ppm and the crystallinity of reacted Pt NPs@MIL-53(Fe) is unchangeable.*

KEYWORDS: *Directing self-assembly; Mono-disperse nano-particle; MIL-53(Fe); Catalytic behavior.*

INTRODUCTION

In the past decades, efforts are devoted to a kind porous material known as the metal-organic framework owing to the potential applications such as gas-storage/gas-separation, drug delivery, chemical sensing, and catalysis and so forth [1-5]. So far, thousands of MOF materials have been prepared, which reveals the diversities of the compositions and structures [6]. Some of MOF materials such as HKUST-1[7], MIL-53[8], MIL-100[9], MIL-101[10], ZIF-8[11] and UIO-66[12] etc., are very enchanted owing to the stabilities involving in the chemical, solvent, water, thermal, light etc. Recently, MOF composites have been attracted more attention, in which MOF can serve as either host or guest to assemble desired material together [13]. The performances of the resulting composite, however, are scarcely explored.

The catalysis is a promising chemical process of MOF not only because of their channel/cavity structure which is constructed by a node of metal ion/ cluster and linker of the organic ligand can offer the place for the chemical reaction [14] but also MOF can accommodate the desired material to form the composite and moreover give rise

***** *To whom correspondence should be addressed.*
+ E-mail: liyafeng@ ccut.edu.cn
1021-9986/2018/3/43-49 *7/$/5.07*

to the expectably catalytic behavior. Usually, MOF materials would not exhibit the catalytic properties because of the neutral framework. However, as the coordinated water in metal sites is removed, the MOF with vacancy metal site might sever as the Lewis-acid catalysis, for example, that HKUST-1 and MIL-101 can catalyze the cyanosilylation of benzaldehyde or acetone [15,16]. Alternatively, MOF materials can serve as the host, which is embedded into by the particles as the active site including the metal, alloy, metal oxide, metal complex and POM etc.[13,17, 18]. Meanwhile, the MOF composites have been carried out by the methods of liquid-impregnation and gas-infiltration [19, 20]. Recently, a new method called as directing self-assemble or templated method has been developed to prepare M or MOx NPs@MOF [18, 21], which is somewhat attributed to the relatively flexible framework of MOF materials. Guang Lu et al have considerably studied the process of DSA preparation of M/MOx/MX NPs@ZIF-8, notably, in which Pt NPs@ZIF-8 exhibits the region-hydrogenation-catalyst [18].

In the case of Pt NPs@ZIF-8, the Pt nanoparticles are dispersed as much as possible inside the ZIF-8 and locked by the lattices of ZIF-8 to effectively avoid aggregation or sinter of particles. However, the aperture of ZIF-8(~3.4Å) is too small to permit the entrance or exit of a bigger molecule. The aperture of the MIL-53 ranges from ~0.8nm to ~1.3nm, which derivates from the called 'breathing' effect. On this level, molecules with ~100Da of formula weight might go in or out freely. Moreover, their chemical reactions, especially on the region-oxidation and region-reduction, have always been the highlight fields by both academic and industrial views. As the catalyst, the noble metal [22] can be prepared large-scale with all sizes. In this work, we have achieved to embed mono-disperse metal nano-particles (2.5nm Pt) into the MIL-53, and furthermore investigated their properties of composites through the catalytic behaviors to thiophene hydrogenation.

EXPERIMENTAL SECTIONS

Synthesis

2.5nm Pt capped by PVP was prepared accordingly to ref. [22] (Supporting Information S1, Fig.S1).

Solvothermal synthesis of MIL-53(Fe) at 80°C. $FeCl_3{\cdot}6H_2O$ (270mg, 1.0mmol, Aladdin) and H_2BDC (1,4-benzene dicarboxylic acid, 249mg, 1.5mmol, Aladdin) were dissolved into DMF (*N,N'*-dimethylformamide, 10ml, 130mmol, Aladdin) to a brown solution. After continuously stirred for half an hour, the mixture with a molar ratio of $FeCl_3{\cdot}6H_2O$: H_2BDC : DMF = 1 : 1.5 : 130 was sealed in an autoclave, put into the CE oven and crystallized at 80°C for 42 hours. The product was centrifugally collected at 6000rpm for 5min, washed three times by ethanol, and dried at 80°C overnight. The yield was ~51.9% (based on the $Fe^{III}(OH)\{O_2C\text{-}C_6H_4\text{-}CO_2\}\cdot H_2O$ [23])

Microwave irradiation synthesis of MIL-53(Fe) at 100°C. $FeCl_3{\cdot}6H_2O$ (90mg, 0.33mmol) and H_2BDC(83mg, 0.5mmol) were dissolved into DMF(40ml, 520mmol) in a simple flask to the brown solution, and continuously stirred for half an hour. Finally, the mixture with a molar ratio of $FeCl_3{\cdot}6H_2O$: H_2BDC : DMF = 1 : 1.5 : 1 560 was put into the microwave oven and irradiated at 100°C for 4 hrs. The product was centrifugally collected at 6000rpm for 5min, washed three times by ethanol, and dried at 80°C overnight. The yield was ~90.1%.

Ultrasound synthesis of MIL-53(Fe) at 70°C. $FeCl_3{\cdot}6H_2O$ (540mg, 2mmol) and H_2BDC(332mg, 2mmol) were dissolved into DMF(10ml, 130mmol) in a flask to the brown solution, and continuously stirred for half an hour. Finally, the mixture with a molar ratio of $FeCl_3{\cdot}6H_2O$: H_2BDC : DMF = 1 : 1 : 65 was put into an ultrasonic generator and sonicated at 70°C for 4 hrs at power 100W. The product was centrifugally collected at 6000rpm for 5min, washed three times by ethanol, and dried at 80°C overnight. The yield was ~16.9%.

Pt NPs@MIL-53(Fe) of 2.5wt% composite was carried out by modifying the amount of nanoparticle.

Catalytic behaviors

Thiophene hydrogenation. The stock solution of thiophene/*n*-octane was prepared by adding 200mg of thiophene (Aladdin) into 1l of *n*-octane (76ppm of S, Aladdin). 50ml of thiophene/*n*-octane solution and 500mg of Pt NPs @MIL-53 were added into the three-neck flask equipped with condenser. The mixture was stirringly heated up to 120°C and retained. H_2 flow was controlled at 10ml/min. The sample was taken every half hour and analyzed by ZWK-2001 Microcomputer Sulfur Chloride Analyzer Instrument.

Materials characterizations

Powder X-ray diffraction (PXRD). Powder X-ray diffraction (PXRD) patterns were recorded on a Rigaku D/MAX PC2200 diffractometer for Cu Kα radiation (λ =1.5406 Å), with a scan speed of 5°/min.

TEM. The morphologies of the samples were inspected on a transmission electron microscope (JEOL-2000ex).

FTIR. The infrared (IR) spectra were recorded within the 400~4000 cm^{-1} region on a Nicolet iS10 FT-IR spectrometer using KBr pellets.

Thermal gravimetric analyses (TG). The thermal gravimetric analyses (TG) were performed on TGA Q5000 instrument used in a nitrogen environment with a heating rate of 10°C/min.

N_2 isothermal adsorption. N_2 isothermal adsorption experiments were performed at 77 K with a V-Sorb 2800P apparatus using nitrogen as the probing gas. The samples were vacuumed for 6hrs at 120°C before the data were collected.

ZWK-2001 Microcomputer Sulfur Chloride Analyzer Instrument. Operated condition: concentration of standard sample (dibutyl sulfide): 150mg/l, conversion: 70~120%; vaporized temperature: 760°C; cracking temperature: 860°C; N_2 flow: 150~200ml/min; O_2 flow: 250~300ml/min; injected volume of sample: 4.4μl.

IRIS Intrepid II ICP instrument (Thermo Electron Corp.). The certain amount of product was filtered by using 0.45μm membrane and dissolved by H_2O_2/H_2SO_4.

RESULTS AND DISCUSSIONS

The effect of the preparation methods on MIL-53(Fe)

The mono-disperse nanoparticle (Pt NPs) is a metastable phase and sensitive to the reaction temperature, so the reaction temperature is as lower as possible in order to avoid the aggregation of mono-disperse nano-particles. In our work, the methods, involving in the CE oven, microwave irradiation and ultrasound, have been tried to prepare the MIL-53 (Fe), and in the meantime, the reaction temperature is definitely ranged from 70 to 100°C. The PXRD shows that MIL-53(Fe)s prepared through different methods consist of ones from ref.[24,25] (Fig.1). From TEM diagrams (Fig.1), the MIL-53(Fe) particles prepared through the different methods are uniform with > 100nm of particle sizes. FT-IR spectroscopy (Supporting information Fig.S2) shows the characteristic vibration bands of the O_2C-C_6H_4-CO_2 and Fe-O in MIL-53(Fe). The thermal stability of MIL-53(Fe)s are determined by the TG (Supporting information Fig.S3), which give rise to a sharp weight loss after 400°C. The surface areas of MIL-53(Fe)s prepared by the different methods are calculated by the N_2 isothermal adsorption at 77K, such as 1044 m^2/g of MIL-53(Fe)-MW-100, 920 m^2/g of MIL-53(Fe)-UTS-70 and 900 m^2/g of MIL-53(Fe)-CE-oven-80 (Supporting information Fig.S4, Table 1).

The effect of the preparation methods on DSA preparation of Pt NPs @ MIL-53(Fe)

Based on the above results, three methods, such as CE-oven-80, MW-100, and UTS-70, have been used to prepare the Pt NPs@MIL-53(Fe), respectively. The PXRD, TEM, FT-IR, TG, and N_2 isothermal adsorption are employed to characterize the obtained Pt NPs@MIL-53(Fe). The results of PXRD show that Pt NPs@MIL-53(Fe) consists with MIL-53(Fe), which means that MIL-53(Fe) framework remain unchanged with Pt nanoparticles embedded into the framework of MIL-53(Fe) (Fig.2). From TEM diagram (Fig.3), the Pt nanoparticles are readily embedded into MIL-53(Fe) to form Pt NPs@MIL-53(Fe) matrix. FT-IR spectroscopy of Pt NPs@MIL-53(Fe) basically consists with MIL-53(Fe) and TG shows that there is sharp weight loss after 400°C which is almost the same as the occasion of the MIL-53(Fe) (Supporting information Fig.S6 & Fig.S7). From N_2 isothermal adsorption at 77K, the BET surface area of Pt NPs@MIL-53(Fe) apparently deceases about 200~300 m^2/g with a comparison to MIL-53(Fe) (Table 1, supporting information Fig.S8). The reason is caused by the collapse and jam of channel resulting from the incorporation of Pt nanoparticles.

The catalytic behavior of Pt@MIL-53(Fe) to thiophene hydrogenation

In order to verify the catalytic behaviors of Pt NPs @MIL-53(Fe) composite, the thiophene hydrogenation has been investigated under 120°C of reaction temperature. Firstly, the adsorption experiment of Pt NPs @MIL-53(Fe) to thiophene shows that 500mg Pt NPs @MIL-53(Fe) can adsorb ~10ppm thiophene (Supporting information, S8). During the experiment of thiophene hydrogenation (Fig.4), the sulfur content with using

Table 1: BET surface area of MIL-53(Fe)s and Pt NPs@MIL-53(Fe)s prepared by the different methods.

Method	MW-100	UTS-70	CE-oven
S_A(MIL-53(Fe)) /(m^2/g)	1044	920	900
S_A(Pt NPs@MIL-53(Fe)) /(m^2/g)	847	685	593

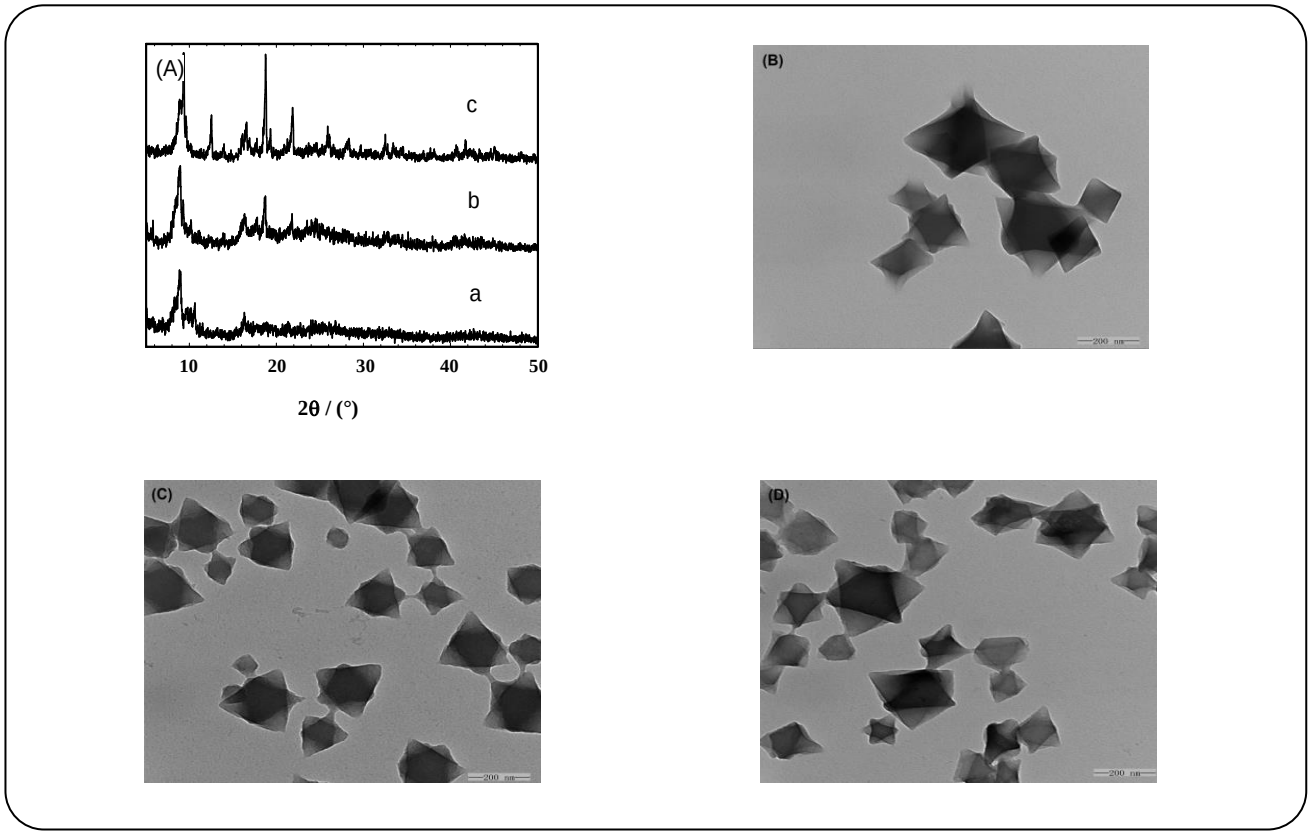

Fig. 1: PXRD patterns (A) and TEM diagrams (B, C and D) of MIL-53(Fe) prepared by the different methods. (A): a. CE oven at 80°C; b. microwave irradiation at 100°C; c. ultrasound at 70°C. (B) CE oven at 80°C. (C) microwave irradiation at 100°C. (D) ultrasound at 70°C.

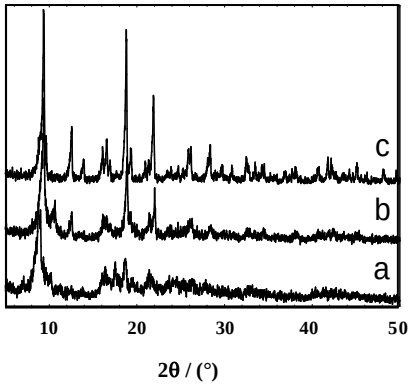

Fig. 2: PXRD patterns of Pt@MIL-53(Fe) prepared by the different methods: a. CE oven at 80°C; b. microwave irradiation at 100°C; c. ultrasound 70°C.

500mg Pt NPs @MIL-53(Fe) as the catalyst rapidly decreases to 8.82ppm in 60min which is far lower than that in the blank. This indicates that Pt NPs @MIL-53(Fe) can efficiently catalyze the thiophene hydrogenation and desulfurize the thiophene. In order to furthermore investigate catalytic properties of Pt NPs @MIL-53(Fe), nitrobenzene and benzothiophene hydrogenations have subsequently been carried out. However, Pt NPs @MIL-53(Fe) does not work to both owing to the shape selectivities of Pt NPs @MIL-53(Fe). After hydrogenation reaction is completed, ICP is utilized to determine the content of Pt in the product. The result shows that no leaching of Pt is found. The stability of

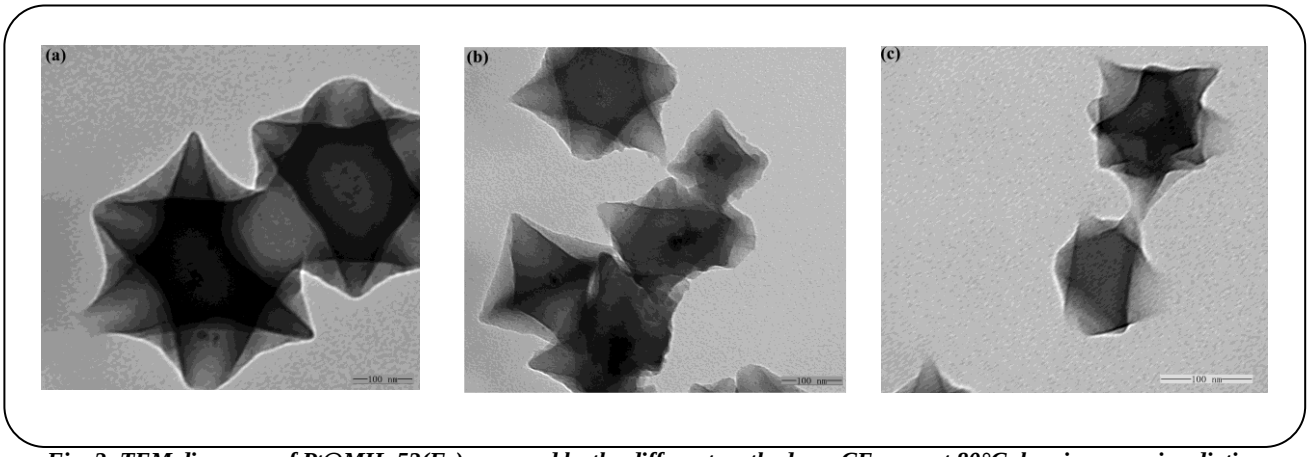

Fig. 3: TEM diagrams of Pt@MIL-53(Fe) prepared by the different methods: a. CE oven at 80°C; b. microwave irradiation at 100°C; c. ultrasound 70°C.

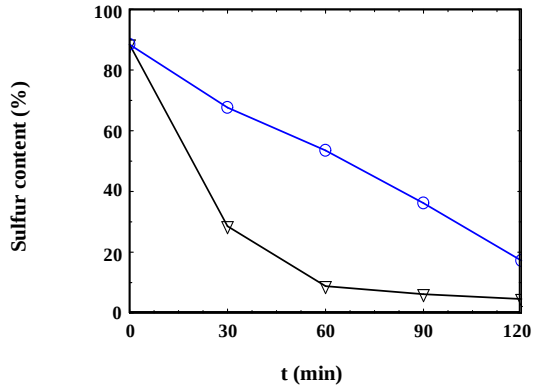

Fig. 4: The curves of sulfur content vs. time. (○) blank; (▽) 500mg Pt NPs@MIL-53(Fe).

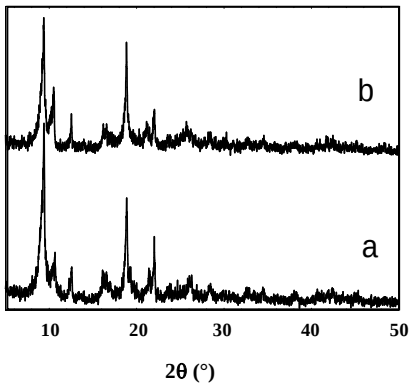

Fig. 5: PXRD patterns of fresh and reacted Pt NPs@MIL-53(Fe). a. fresh; b. reacted.

Pt NPs @MIL-53(Fe) is confirmed by comparing the PXRDs of fresh and reacted Pt NPs @MIL-53(Fe). The results show that the peak intensity and peak shape of both almost consist with each other (Fig.5), which shows the thermal stability of Pt NPs @MIL-53(Fe). The recyclability of Pt NPs @MIL-53(Fe) composite is carried out under the same reaction condition with thiophene hydrogenation. The sulfur content just declines a little after 5 runs, owing to the operating loss of Pt NPs @MIL-53(Fe) (Fig.6).

CONCLUSIONS

In conclusion, different attempts have been used to prepare Pt NPs@MIL-53(Fe), such as CE oven, microwave irradiation, and ultrasound. Consequently, Pt NPs@MIL-53(Fe) prepared by microwave irradiation exhibits uniformed morphology, high crystallinity, and high-disperse Pt NPs, which has been confirmed by FTIR, TG, N_2 adsorption at 77K, TEM and PXRD. Pt NPs@MIL-53(Fe) composite can selectively catalyze the thiophene hydrogenation over benzothiophene hydrogenation. The result shows that the sulfur amount can be reduced to less than 10ppm and the crystallinity of reacted Pt NPs@MIL-53(Fe) is unchangeable.

Acknowledgment

This project is supported by the Scientific Research Foundation for the Returned Overseas Team, Chinese Education Ministry.

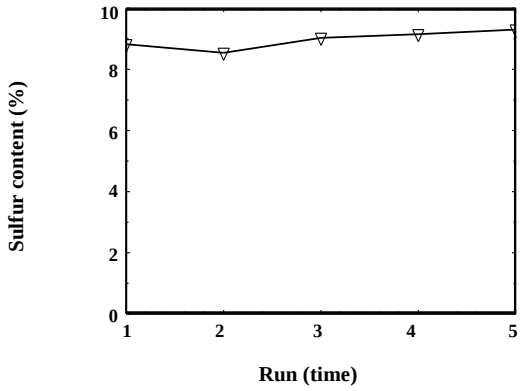

Fig. 6: The recyclability of Pt NPs@MIL-53(Fe).

Received : Aug. 25, 2016 ; Accepted : Oct. 16, 2017

REFERENCES

[1] Suh M.P., Park H.J., Prasad T.K., Lim D.W., Hydrogen Storage in Metal-Organic Frameworks, *Chem. Rev.*, **112:** 782–835(2012).

[2] Sumida K., Rogow D.L., Mason J.A., McDonald T.M., Bloch E.D., Herm Z.R., Bae T.H., Long J.R., Carbon Dioxide Capture in Metal-Organic Frameworks, *Chem. Rev.*, **112:** 724–781 (2012).

[3] Kreno L.E., Leong K., Farha O.K., Allendorf M., Van Duyne R.P., Hupp J.T., Metal-Organic Framework Materials as Chemical Sensor, *Chem. Rev.*, **112:**1105–1125 (2012).

[4] Horcajada P., Gref R., Baati T., Allan P.K., Maurin G., Couvreur P., Férey G., Morris R.E., Serre C., Metal-Organic Frameworks in Biomedicine, *Chem. Rev.*, **112:** 1232–1268(2012).

[5] Lee J.Y., Farha O.K., Roberts J., Scheidt K.A., Nguyen S.B.T., Hupp J.T., Metal–Organic Framework Materials as Catalysts, *Chem. Soc. Rev.*, **38:** 1450–1459(2009).

[6] Tranchemontagne D.J., Mendoza-Cortés J.L., O'Keeffe M., Yaghi O.M., Secondary Building Units, Nets and Bonding in the Chemistry of Metal–Organic Frameworks, *Chem. Soc. Rev.*, **38:** 1257–1283(2009).

[7] Stephen S.Y.C., Samuel M.F.L., Jonathan P.H.C., Orpen A.G., Williams I.D., A Chemically Functionalizable Nanoporous Material $[Cu_3(TMA)_2(H_2O)_3]_n$, *Science*, **283:** 1148-1150(1999).

[8] Serre C., Millange F., Thouvenot C., Noguès M., Marsolier G., Louër D., Férey G., Very Large Breathing Effect in the First Nanoporous Chromium(III)- Based Solids: MIL-53 or $Cr^{III}(OH)\cdot\{O_2C-C_6H_4-CO_2\}\cdot\{HO_2C-C_6H_4-CO_2H\}_x\cdot(H_2O)_y$, *J. Am. Chem. Soc.*, **124**(45): 13519-13526(2002).

[9] Horcajada P., Serre C., Vallet-Regí M., Sebban M., Taulelle F., Férey G., Metal–Organic Frameworks as Efficient Materials for Drug Delivery, *Angew. Chem. Int. Ed.*, **45**(36): 5974–5978(2006).

[10] Férey G., Mellot-Draznieks C., Serre C., Millange F., Dutour J., Surblé S., Margiolaki I., A Chromium Terephthalate–Based Solid with Unusually Large Pore Volumes and Surface Area, *Science*, **309:** 2040-2042(2005).

[11] Huang X.C., Lin Y.Y., Zhang J.P., Chen X.X., Ligand-Directed Strategy for Zeolite-Type Metal-Organic Frameworks: Zinc(II) Imidazolates with Unusual Zeolitic Topologies, *Angew. Chem. Int. Ed.*, **45**: 1557–1559(2006); Park K.S., Ni Z., Côté A.P., Choi J.Y., Huang R.D., Uribe-Romo F.J., Chae H.K., O'Keeffe M., Yaghi O.M., Exceptional Chemical and Thermal Stability of Zeolitic Imidazolate Frameworks, *PNAS*, **103**(27): 10186–10191(2006).

[12] Cavka J.H., Jakobsen S., Olsbye U., Guillou N., Lamberti C., Bordiga S., Lillerud L.P., A New Zirconium Inorganic Building Brick forming Metal Organic Frameworks with Exceptional Stability, *J. Am. Chem. Soc.*, **130:** 13850–13851(2008).

[13] Zhu Q.L., Xu Q., Metal–Organic Framework Composites, *Chem. Soc. Rev.*, **43:** 5468-5512 (2014); Shen L., Wu W., Liang R., Lin R., Wu L., Highly Dispersed Palladium Nanoparticles Anchored on UiO-66(NH_2) Metal-Organic Framework as a Reusable and Dual Functional Visible-Light-Driven Photocatalyst, *Nanoscale*, **5**: 9374-9382 (2013); He J., Yan Z., Wang J., Xie J,, Jiang L., Shi Y., Yuan F., Yu F., Sun Y., Significantly Enhanced Potocatalytic Hydrogen Evolution under Visible Light over CdS Embedded on Metal–Organic Frameworks, *Chem. Commun.*, **49:** 6761-6763 (2013); Zhao M., Deng K., He L., Liu Y., Li G., Zhao H., Tang Z., Core–Shell Palladium Nanoparticle@Metal–Organic Frameworks as Multifunctional Catalysts for Cascade Reactions, *J. Am. Chem. Soc.*, **136:** 1738-1741(2014).

[14] Czaja A.U., Trukhan N., Müller U., Industrial Applications of Metal–Organic Frameworks, *Chem. Soc. Rev.*, **38:** 1284–1293(2009).

[15] Schlichte K., Kratzke T., Kaskel S., Improved Synthesis, Thermal Stability and Catalytic Properties of the Metal-Organic Framework Compound $Cu_3(BTC)_2$, *Microporous Mesoporous Mater.*, **73:** 81–88(2004).

[16] Henschel A., Gedrich K., Kraehnert R., Kaskel S., Catalytic Properties of MIL-101, *Chem. Commun.*, 4192–4194(2008).

[17] Dhakshinamoorthy A., Garcia H., Catalysis by Metal Nanoparticles Embedded on Metal–Organic Frameworks, *Chem. Soc. Rev.*, **41:** 5262–5284(2012).

[18] Lu G. Li S.Z., Guo Z., Farha O.K., Hauser B.G., Qi X.Y., Wang Y., Wang X., Han S.Y., Liu X.G., DuChene J.S., Zhang H., Zhang Q.C., Chen X.D., Ma J., Loo S.C.J., Wei W.D., Yang Y.H., Hupp J.T., Huo F.W., Imparting Functionality to a Metal–Organic Framework Material by Controlled Nanoparticle Encapsulation, *Nat. Chem.*, **4:** 310–316(2012).

[19] Ameloot R., Roeffaers M.B.J., Cremer G.D., Vermoortele F., Hofkens J., Sels B.F., Vos D.D., Metal–Organic Framework Single Crystals as Photoactive Matrices for the Generation of Metallic Microstructures, *Adv. Mater.*, **23:** 1788-1791 (2011).

[20] Hermes S., Schröter M.K., Schmid R., Khodeir L., Muhler M., Tissler A., Fischer R.W., Fischer R.A., Metal@MOF: Loading of Highly Porous Coordination Polymers Host Lattices by Metal Organic Chemical Vapor Deposition, *Angew. Chem. Int. Ed.*, **44:** 6237–6241(2005).

[21] Tsuruoka T., Kawasaki H., Nawafune H., Akamatsu K., Controlled Self-Assembly of Metal–Organic Frameworks on Metal Nanoparticles for Efficient Synthesis of Hybrid Nanostructures, *ACS Appl. Mater. Interfaces*, **3:** 3788-3791(2011).

[22] Rioux R.M., Song H., Hoefelmeyer J.D., Yang P., Somorjai G.A., High-Surface-Area Catalyst Design: Synthesis, Characterization, and Reaction Studies of Platinum Nanoparticles in Mesoporous SBA-15 Silica, *J. Phys. Chem. B*, **109:** 2192-2202(2005).

[23] Férey G., Millange F., Morcrette M., Serre C., Doublet M.L., Grenèche J.M., Tarascon J.M., Mixed-Valence Li/Fe-Based Metal–Organic Frameworks with Both Reversible Redox and Sorption Properties, *Angew. Chem. Int. Ed.*, **46:** 3259-3263(2007); Horcajada P., Serre C., Maurin G., Ramsahye N.A., Balas F., Vallet-Regí M., Sebban M., Taulelle F., Férey G., Flexible Porous Metal-Organic Frameworks For a Controlled Drug Delivery, *J. Am. Chem. Soc*., **130:** 6774-6780(2008).

[24] Gordon J., Kazemian H., Rohani S., Rapid and Efficient Crystallization of MIL-53(Fe) by Ultrasound and Microwave Irradiation, *Microporous and Mesoporous Mater*., **162:** 36-43 (2012).

[25] Ai L., Li L., Zhang C., Fu J., Jiang J., MIL-53(Fe): A Metal–Organic Framework with Intrinsic Peroxidase-Like Catalytic Activity for Clorimetric Biosensing, *Chemistry-A Eur. J.*, **19:** 15105-15108(2013).